UNLIMITED

RSRE
MEMORANDUM No. 4363

ROYAL SIGNALS & RADAR ESTABLISHMENT

QUANTUM WELL INFRA-RED DETECTORS I: SOME CALCULATIONS OF THEIR OPTICAL PROPERTIES

Author: M J Kane

PROCUREMENT EXECUTIVE,
MINISTRY OF DEFENCE,
R S R E MALVERN,
WORCS.

UNLIMITED

0071470

CONDITIONS OF RELEASE

BR-113883

....

DRIC U

....

DRIC Y

Reports quoted are not necessarily available to members of the public or to commercial organisations.

ROYAL SIGNALS AND RADAR ESTABLISHMENT

Memorandum 4363

TITLE: QUANTUM WELL INFRA-RED DETECTORS I:

SOME CALCULATIONS OF THEIR OPTICAL PROPERTIES

AUTHOR: M J KANE

SECTION HEAD: N APSLEY

DATE: FEBRUARY 1990

SUMMARY

The quantum well infrared detector is a new kind of infrared photon detector that can be made to work in the wavelength range 5 to 20 μm. This memorandum describes some theoretical calculations which illustrate the mode of operation of this detector. The initial part of the memo describes qualitatively the manner in which a quantum well system can be made into an infrared photoconductor and illustrates the optical processes in such a device with some calculations of the properties of an idealised system. The second half of the memo concentrates on including some of the corrections necessary to give an accurate description of a real quantum well system and presents the design rules necessary to give a detector with a specified threshold photon energy.

Keywords: Infrared detectors; Quantum theory; Optical properties, (CP)

1 An introduction to the quantum well infra red detector

The quantum well infrared detector is a new kind of infra-red photon detector. The detector is fabricated from multilayer structures of compound semiconductors. The detector can be made to work in any 100 meV wide window with a low energy threshold in the range 50 to 200 meV (this corresponds to a wavelength range of 5 to 20 microns) when made from GaAs/AlGaAs. The use of other related materials such as InGaAs would widen this range somewhat. Detectors for use in this wavelength region are usually made from highly specialized materials systems such as $Hg_xCd_{1-x}Te$ or InSb and are therefore difficult to integrate with other forms of electronics. The quantum well detectors are fabricated from GaAs/AlGaAs epitaxial structures which are normally grown on large wafers (>2 inch diameter). The fabrication process always produces large arrays of detectors whose properties are uniform across the wafer. The processing methods used to make the quantum well infra red detector are similar to those used to make other GaAs devices and it is therefore possible to conceive of monolithically integrating signal processing and control electronics with the detectors. It should also be possible to grow quantum well infrared detectors on GaAs layers grown on silicon and thereby allow integration with silicon devices.

The detectors show high detectivity and high operating speeds. The first detectivitiy measurement was 10^{10} cm$\sqrt{\text{Hz}}$W^{-1} for a detector with a peak response at 8 microns wavelength working at a temperature of 77K[1]. Subsequently, similar detectivities were obtained in a detector with a peak responsivity at 10 microns microns albeit at a relatively low working temperature of 50K[2]. This detectivity was measured with a 180° field of view of room temperature black body radiation and is background limited. Response time faster than 300 pS have been measured[3].

The quantum well infra-red detector was pioneered by Levine and colleagues of AT and T Bell laboratories who have produced many publications on the topic. (See for example references 1 to 3 and the other papers cited therein.) However, their papers

tend to describe results on individual device structures in isolation without any attempt to provide any overview or synthesis. The purpose of this note is to describe calculations relevant to a number of different aspects of the operation of the QWIR detector and aims to go some way to providing this synthesis.

This note is organised as follows: It begins (in section 2) by describing the optical absorption process, intersubband absorption, which underlies the operation of the quantum well infrared detector and establishes the particular conditions under which intersubband absorption can be described as a bound to free process. (In a bound to free process the excited state is more mobile than the ground state, a necessary prerequisite for the construction of a photoconductor.) Section 3 shows how to calculate the strength of the bound to free absorption in a simple parabolic semiconductor system. Section 4 extends some of these ideas to include a more realistic model of a semiconductor in which nonparabolicity is taken into account. This section concentrates on the type of calculation necessary in order to determine the materials parameters necessary to specify a real structure in which bound to free transitions with a given threshold energy are the dominant intersubband absorption process. This completes the aim of the memorandum, i.e. it enables one to construct a first pass specification for a QWIR detector working a given wavelength.

2 Intersubband absorption in infinite and finite depth quantum wells

(i) Intersubband absorption in an infinitely deep quantum well.

When a particle of mass m^* (typically an electron in a semiconductor where parabolic effective mass theory is applicable,) is confined in an infinitely deep rectangular potential well of width a there are an infinite number of quantised energy levels. The energy of the n^{th} quantised level is given by the formula

$$E_n = \frac{\hbar^2 \pi^2 n^2}{2m^* a^2} \tag{1}$$

An energy level diagram is shown in figure 1. Electric dipole transitions between any two levels of different parity can be excited by an electric field oscillating perpendicular to the plane of the quantum well. The strength of any absorption is proportional to the number of electrons in the ground state of the transition. In most cases the only energy level that can have a significant population is the ground state of the system with index n=1. The integral of the absorption coefficient, $\alpha(\omega)$, across the lineshape of the transition from the n=1 state to the n=i state can be shown to satisfy the relation:

$$\int \alpha(\omega)\, d\omega \propto f_{1i} n_{gs} \tag{2}$$

where ω is the angular frequency and f_{1i} is the oscillator strength, which defined by the relation:

$$f_{ji} = \frac{2m^*}{\hbar} (\omega_i - \omega_j) \left| \langle j | z | i \rangle \right|^2 \tag{3}$$

where j is the index of the initial state and i is the index of final state. (j=1 for the case that is of particular interest here.) The oscillator strength satisfies the Thomas Reiche Kuhn sum rule

$$\sum_i f_{ji} = 1 \tag{4}$$

In an infinitely deep quantum well the the dependences of f_{ji} on all the various material parameters cancel and the oscillator strength is a function of i and j only and has the

1 Infinitely deep potential well

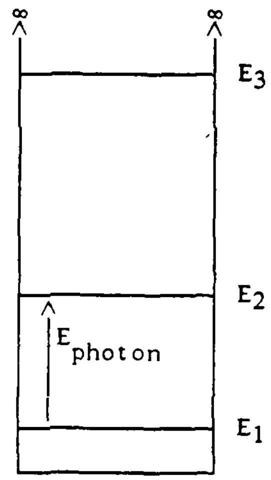

Figure 1 An energy level diagram for an infinitely deep quantum well showing the dominant intersubband transition from the ground state.

value;

$$f_{ji} = \frac{64}{\pi^2} \frac{j^2 i^2}{(j^2 - i^2)^3} \tag{5}$$

Using equation (5) it is easily shown that $f_{21} = 0.96$ and thus that although transitions are allowed between the n=1 level and any level with an even index only absorption to the n=2 level makes a significant contribution to the oscillator strength.

(ii) Finite depth quantum wells

No real quantum well system can have an infinite well depth, so we will now consider a finite depth quantum well and show, in the first place descriptively, that this is what is needed for a quantum well infra red detector.

An energy level diagram for a finite depth well is shown in figure 2. It can be seen that there is a continuum of unbound states at energies above the barrier height and a finite number of confined states at energies below the barrier height. The results of a calculation of the energy levels in a finite well as a function of well width are shown in figure 3. It can be seen that the number of bound states in the well decreases as the well width decreases but that there is always one bound state in the well.

Although the transition of a particular state from being bound to being unbound occurs at a discrete energy, the wavefunction of the state concerned makes a much more gradual change. The wings of the wavefunction penetrate into the barriers to an increasing degree such that the state gradually becomes completely delocalized. When a "bound" state has an energy equal to the top of the well, the wavefunction in the barrier has a decay constant of zero i.e. the wavefunction neither grows nor decays. In order to match this wavefunction with that in the well it is found that the well width must be such that the well contain an exact number of half wavelengths of the electron wavefunction. This means that the bound state in the well changes continuously into a resonance in the continuum above the top of the well. (The condition for a resonance is again that an exact number of half wavelengths of the electron wavefunction fit into the well. However, a resonance is normally thought of as being a state with an energy significantly greater than the top of the well.)

2 Finite potential well

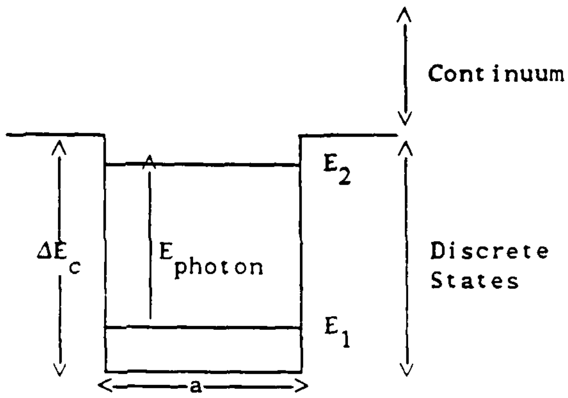

Figure 2 an energy level diagram for a finite depth quantum well showing the dominant intersubband transition and the energy regimes where discrete states and continuum states can be found.

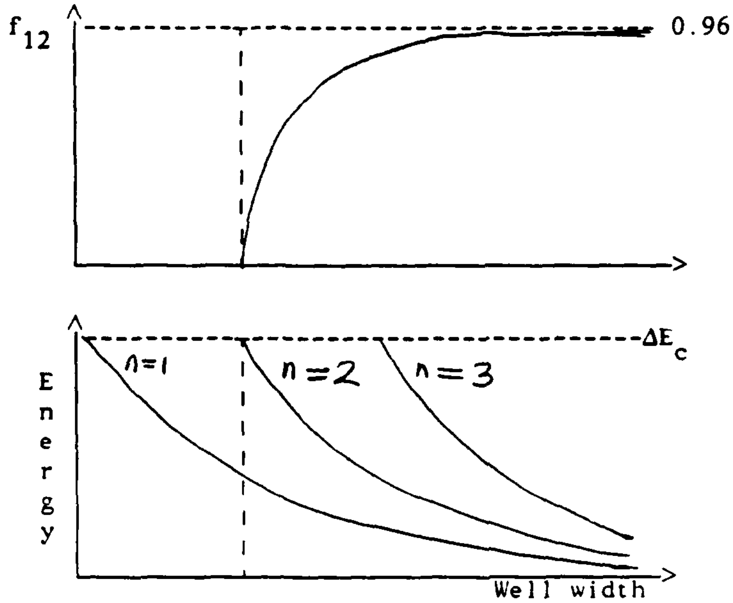

Figure 3 A schematic depiction of the energy levels and oscillator strength of the n=1 to n=2 transition in a finite depth quantum well and a function of well depth.

At this point it is convenient to note that the number of bound states, N_{well}, is given by the simple formula :

$$N_{well} = 1 + \mathrm{Int}(k(\Delta E_c)a/\pi) \qquad (6)$$

where $k(\Delta E_c)$ is the wavevector of an electron with an energy equivalent to the top of the well.

Figure 3 also shows the oscillator strength of the n=1 to n=2 transition as a function of the well width. As the well width decreases the wavefunction of the n=2 states penetrates into the barriers more rapidly than that of the n=1 state. The dipole matrix element and hence the oscillator strength between the two states decreases and becomes zero when the n=2 state becomes unbound. However, the sum rule of equation (4) above show that the sum of the oscilator strength over all possible final states must still be unity. This means that as the oscillator strength of the n=1 to n=2 transition decreases, oscillator strength must transferred to transitions from the n=1 state to states in the continuum above the top of the well. The total oscillator strength in the bound to free transition is maximised if there is only one bound state in the well. The bound to free absorption is always dominated by states just above the top of the well because this is where there is a large density of final states. (This will be illustrated quantuitatively in section 3)

The excited state of a bound to free transition will be mobile perpendicular to the plane of the quantum well. This means that bound to free absorption can be the basis of a photoconductive detector. All that is necessary is to have contacts either side of the quantum well which can apply a bias and collect the photoexcited electrons.

(iii) The effect of doping on the intersubband absorption

Equation (2) shows that the the strength of the intersubband absorption is directly proportional to the density of the electrons in the quantum wells. The doping densities required to obtain a significant intersubband absorption results in an electron gas that is degenerate, i.e. the Fermi energy is significantly greater than the thermal energy k_BT. When a photon is absorbed in an intersubband process the initial state of the electron can have any value up to the Fermi energy. This energy range represents different states of motion of the electrons in the plane of the quantum well whereas the

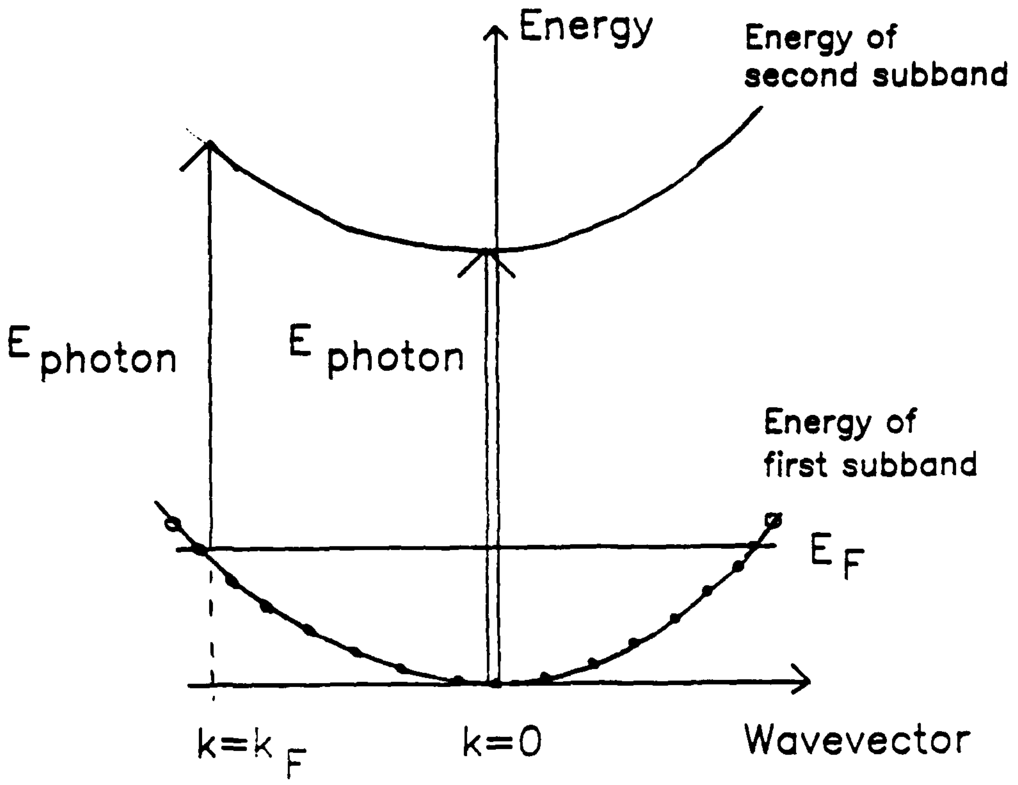

Figure 4 The dispersion of the two subbands in a quantum well. The range of possible intersubband transitions are shown by the vertical arrows. Photons carry very little momentum so that the absorption of a photon causes very little change in wavevector. In a parabolic system the two dispersion curves are parallel so that the transition energy is the same for both an electron excited from the Fermi wavevector and an electron excited from k=0.

intersubband absorption represents a change in the motion of the electron perpendicular to the well. These two processes are to a first approximation independent and the energy required for the intersubband absorption is independent of the initial state of the electron. This is illustrated more clearly by a consideration of the dispersion of the two lowest subbands in a quantum well is shown in figure 4. Photons carry very little momentum so that optical absorption occurs between two states with the same in plane wavevector. In a perfectly parabolic system the energy separation bvetween the two subbands is the same at $k=0$ and at $k=k_F$ so that the dispersion does not broaden the absorption linewidth. In a real system the in-plane masses of the two subbands will be different and the dispersion will cause a broadening of the order $E_F(1-m_1/m_2)$ where m_1 and m_2 are the in-plane effective masses of the two different subbands.

3 Optical properties: calculation of absorption coefficient for bound to free absorption in a parabolic system.

This section describes how to calculate the absorption coefficient of a homogeneous medium entirely filled with quantum well for light whose polarization is such that it is subject to intersubband absorption. In order to model the optical properties of a multiple quantum well structure it is necessary to contruct the full anisotropic dielectric response function of the quantum well by both allowing for the free electron nature of the electron response in the plane of the quantum well and by Kramers Kronig transforming the intersubband absorption in order the obtain the real part of the perpendicular component of the dielectric function. The quantum wells must then be embedded in a multilayer model of the complete system. However, a rough estimate of the absorption coefficient that will be measured can be obtained by taking the homogeneous absorption coefficient and diluting it in proportion to the resolved component of the electric field with the appropriate polarization and the well to barrier mark space ratio.

The main purpose of this section is to illustrate in a rather more quantitative manner than the previous section the way in which the total bound to free absorption changes as the n=2 bound state becomes unbound. The only contribution towards a non zero linewidth in the calculation reported above is the continuous distribution of the final states of the transition. In reality there will be other contributions to the linewidth from factors such as inhomogoneous broadening, lifetime broadening, and nonparabolicity. These factors will not be discussed further here.

The absorption coefficient for the bound-to-free transition in the homogeneous medium can be calculated using the Fermi golden rule

$$W = \frac{2\pi}{\hbar} |\langle\psi_1|V|\psi_2\rangle|^2 g(E) \tag{1}$$

where W is the transition rate, V is the time independent part of the interaction Hamiltonian, ψ_1 and ψ_2 are the wavefunctions for the ground and excited states respectively, E is the energy difference between the ground and excited states and g(E) is the joint density of states between the initial and final states at the transition energy. The absorption coefficient A is obtained from the relation

$$A = \frac{W\hbar\omega}{I} \tag{2}$$

where $\hbar\omega$ is the incident photon energy and I is the incident light intensity, $n_r\epsilon_0 E^2/2c$. E is the z component of the electric field of the light. This simplifies to

$$A = \frac{16\pi^2}{n_r} \hbar\omega N_{3d} g^*(E) \left|\langle\psi_1\left|V\right|\psi_2\rangle\right|^2 \tag{3}$$

where α is the fine structure constant ($\simeq$1/137) and N_{3d} is the bulk electron density in the well. n_r is the refractive index of the medium. The term $g^*(E)$ is the one–dimensional density of states in the excited state. The term $g^*(E)N_{3d}$ is obtained by integrating the product of electron distribution function and the joint density of states over the possible motions of the electrons in the plane of the quantum well and normalising to unit quantum well thickness. The in–plane effective mass of the electron is assumed to be the same for both the ground state and the excited state so that there is no broadening of the absorption.

The wavefunction ψ_1 is the symmetric ground state wavefunction of the quantum well which has the form

$$\begin{aligned} \psi_1 &= B\cos(k_w x) & \left|x\right| &< \tfrac{a}{2} \\ &= C\exp(-\left|K_b\right|x) & \left|x\right| &> \tfrac{a}{2} \end{aligned} \tag{4}$$

where $(k_w)^2 = 2m_w(V+E)/\hbar^2$, $(K_b)^2 = -2m_b E/\hbar^2$, a is the well width m_b and m_w are the effective masses in the barrier and well respectively and V is the well depth. E is the energy of the state with respect to the top of the quantum well. (E is negative for a bound state.)

The bound state energies are given by the solutions to the equation

$$\tan\left[\frac{k_w a}{2}\right] = \frac{K_b m_w}{k_w m_b} \tag{5}$$

The solutions to this equation describe all the symmetric bound states. The antisymmetric states are found by replacing $\tan(k_w a/2)$ in the LHS by $-\cot(k_w a/2)$. The properties of finite square wells are considered by many quantum mechanics text books and we will not say much further here. However we will note that there is always at least one bound state

in the quantum well and that n^{th} bound state reaches the top of a finite depth well when it has the width which would give the $n-1^{th}$ state of an infinite well an energy equivalent to the top of the well. The values of B and C are readily calculated using the normalization condition on the wavefunction.

The wavefunction of the excited stated ψ_2 is forced to be antisymmetric and taken to be

$$\psi_2 = D\sin\left[k_w x\right] \qquad |x| < \frac{a}{2}$$

$$= \left[\frac{2}{L}\right]^{\frac{1}{2}} \sin\left[k_b(x - \frac{a}{2}) + \varphi\right] \qquad |x| > \frac{a}{2} \qquad (6)$$

where $$D^2 = \frac{2}{L}\left[\sin^2\left[\frac{k_w a}{2}\right] + \frac{m_b^2 k_w^2}{m_w^2 k_b^2}\cos^2\left[\frac{k_w a}{2}\right]\right]^{-1}$$

and $$\varphi = \tan^{-1}\left[\frac{m_w k_b}{m_b k_w}\tan\left[\frac{k_w a}{2}\right]\right]$$

where L is the width of the whole system. (It is assumed that the presence of the quantum well does not effect the normalisation of the wavefunction over the whole system.) The amplitude of the wavefunction in the well D oscillates with the energy of the electron above the top of the well between maxima of $(2/L)^{\frac{1}{2}}$ and minima of $(2/L)^{\frac{1}{2}}(E/(V+E))$. The amplitude of the wavefunction in the well for an electron at the top of the well is zero provided that $\cos(k_w a/2)$ is not zero at the top of the well. However, $\cos(k_w a/2)=0$ at the top of the well is the condition that the first excited state is exactly at the top of the well. When this condition is satisfied $D=(2/L)^{\frac{1}{2}}$ at the top of the well. The the behaviour of the mathematical function describing the wavefunction amplitude is rather pathological at this well width and infinitesimal deviations of the well width from that which has the bound state at the top of the well cause the wavefunction amplitude to drop to zero at the top of the well. In practice, finite size effects and scattering would smear out this pathological behaviour.

The density of states is calculated as follows: we require the wavefunction of the excited stated to vanish at $x=L/2$ so that

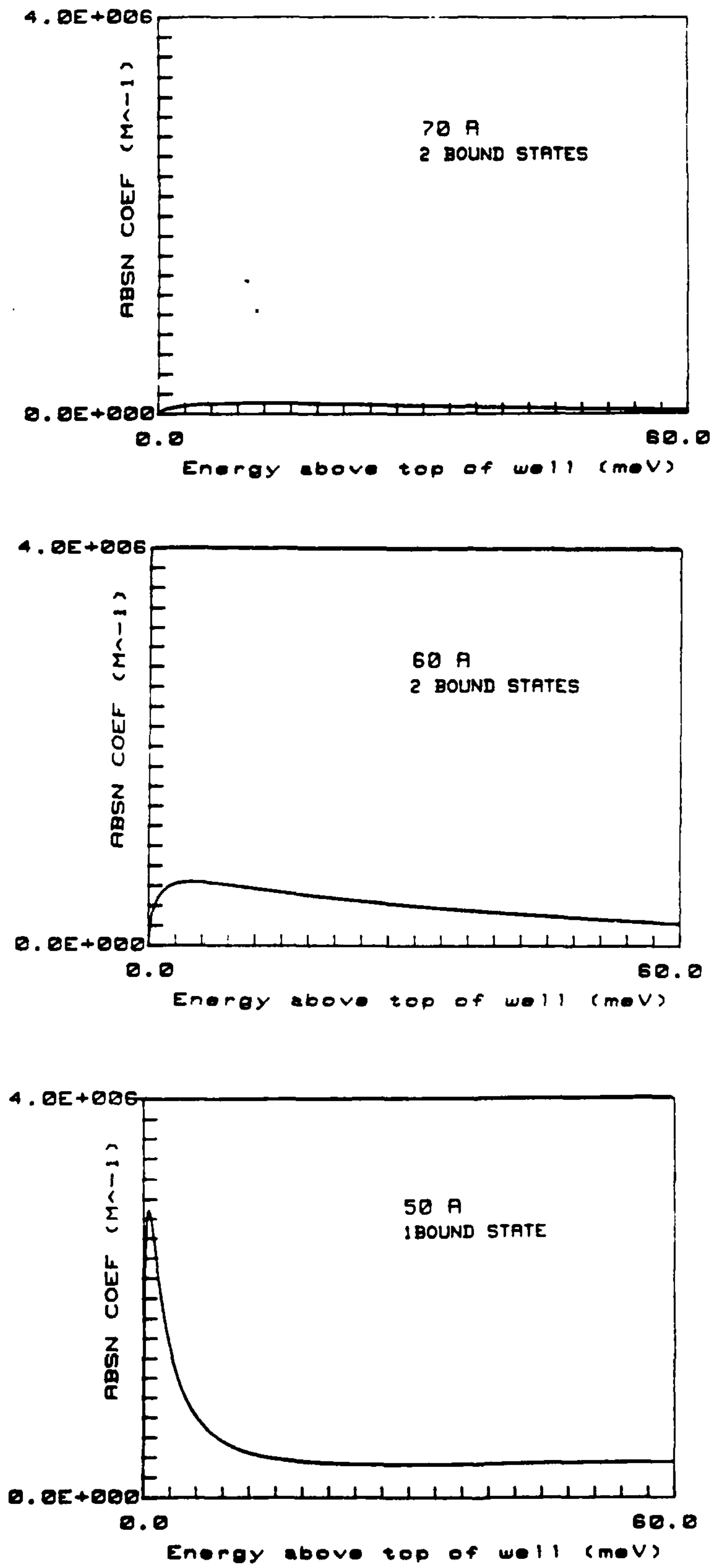

Figure 5 The absorption spectra of the bound to free transitions as a function of the energy of the final state above the top of the well. The spectra are shown for a range well widths with both 1 and 2 bound states in the well. The conduction band offset is 200 meV, the well mass is 0.067 and the barrier mass is 0.1. The conduction band is assumed to be perfectly parabolic. The increase in the total bound to free absorption as the n=2 state becomes unbound is clearly seen.

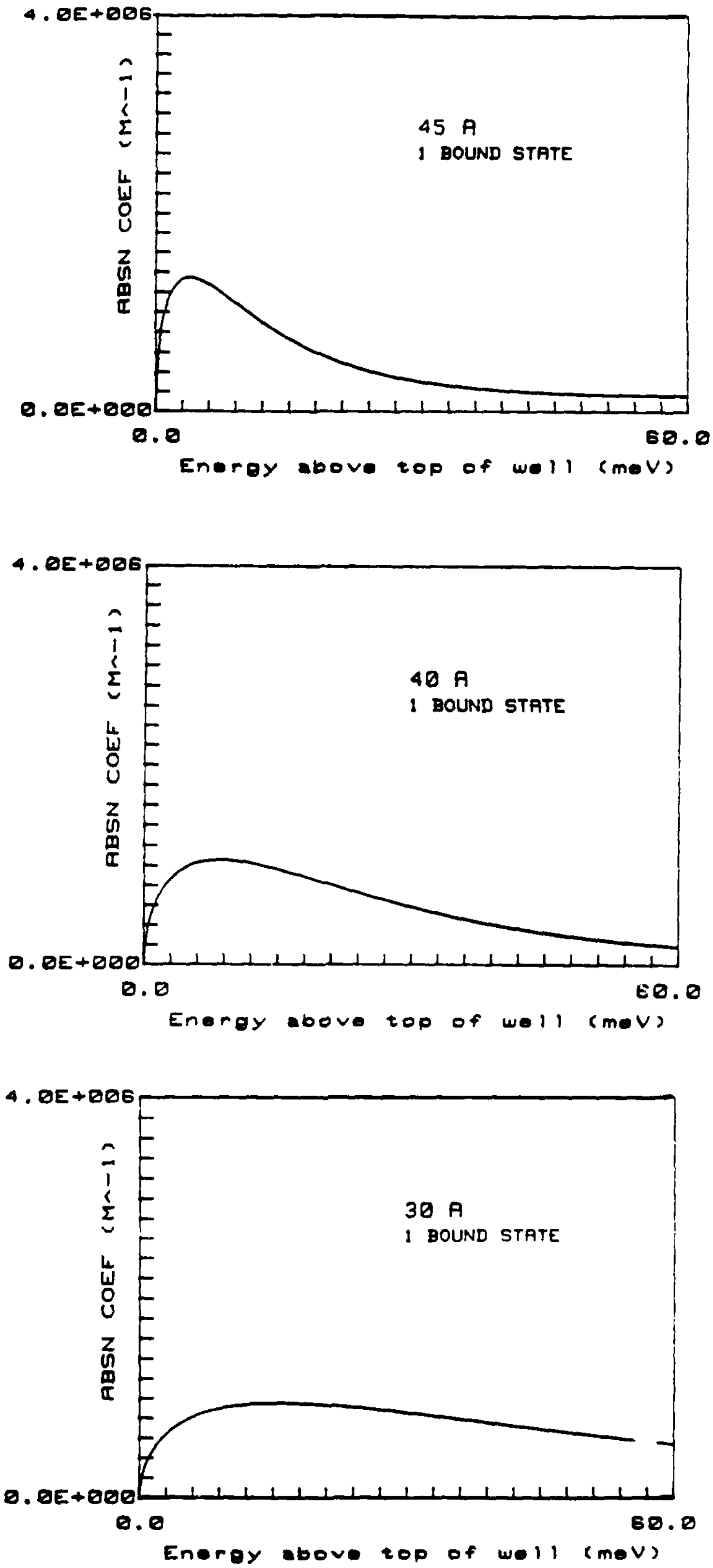

Figure 5 (Continued.) This part of the figure shows the evolution of the bound to free absorption spectrum as the well width is reduced below the point at which the n=2 state becomes unbound.

$$\frac{kL}{2} + \varphi = n\pi \tag{7}$$

and

$$\Delta k = \frac{2\pi}{L} \tag{8}$$

using $E=\hbar^2k^2/2m$ and allowing for spin degeneracy we see that

$$g(E) = \frac{L}{\pi}\frac{m_b}{\hbar}\left[2m_bE\right]^{-\frac{1}{2}} \tag{9}$$

Note that by requiring antisymmetric states we effectively throw away half the possible states. This density of states has the divergence at zero energy characteristic of one dimensional systems.

We now have all of the component parts necessary to calculate the absorption coefficient as given by equation (3). Some typical results are shown in figure 5 for various well widths in a system where the material parameters are chosen to mimic $Al_xGa_{1-x}As/GaAs$ with x=.26 but with no account of non parabolicity. The free electron density is $10^{24}m^{-3}$. It is clearly seen that a strong bound to free absorption is only seen when there is only one bound state in the quantum well and all of the oscillator strength can be found in the bound to free transitions. When there are two tightly bound states in the well (as is the case for a well width of 70 A) there is almost no bound to free absorption. As the well narrows and the second state starts to become unbound, oscillator strength transfers to the continuum and the total strength of the bound to free absorption becomes stronger. The integrated strength of the bound to free absorption becomes constant when there is only one bound state in the well. Making the well narrower than the critical thickness at which the n=2 state becomes unbound tends to push the peak of the bound to free absorption further above the top of the well.

The absorption is particularly peaked (FWHM <1meV) when the well width is close to that for which the second bound state just becomes unbound (≃ 52A). The range of well widths over which this very peaked behaviour occurs is very narrow, far less than a monolayer, and thus never likely to be seen. (Calculations of this behaviour are not shown in figure 5 because of their unphysical nature.)

In practice the linewidth of the bound to free absorption is considerably broader than that obtained from a consideration of the density of final states only, so that the peak value of the absorption coefficient is less than that obtained here.

4 Bound to free absorption in a non parabolic system

The previous section described calculations for a perfectly parabolic system. In practice, quantum well infra red detectors rely on states that sufficiently high inthe conduction band of the GaAs for nonparabolicity to cause significant corrections to their working wavelength. This section will describe a method for calculating the energy levels of a quantum well system in the regime where non parabolicity is significant. We have chosen the semi-empirical envelope function model of Nelson et al. In this calculational scheme a fairly simple model of the band structure is used and then fitted to the measured behaviour of the relevant materials. This appears to give somewhat better results than more complicated first principles models which do not reproduce the measured behaviour of the bulk materials as well as the semi-empirical model.

In the semi-empirical envelope function model the dispersion relation for an electron in the conduction band of GaAs is taken to be :

$$E = \frac{\hbar^2 k^2}{2m^*(E)} \tag{10}$$

where

$$m^*(E) = m_0^*(1+E/E_g) \tag{11}$$

m_0 is the band edge effective mass and E_g is an effective band gap which is chosen match the nonoparabolicity at the band edge to that obtained from a five band bulk crystal model and described by the equation

$$E= \frac{\hbar^2 k^2}{2m^*}(1-\gamma k^2) \tag{12}$$

with γ=4.9 x 10^{-19} m^2. The effective gap is then related to γ by the equation

$$E_g = \frac{\hbar^2}{2m^*\gamma} \tag{13}$$

The nonparabolicity factors in the well and barrier are assumed to be related by the equation

$$\frac{\gamma_w}{\gamma_b} = \left[\frac{m_b^*}{m_w^*}\right]^2 \tag{14}$$

so that an effective gap can be determined from equation (13). The Γ band gap diiference between GaAs and $Al_xGa_{1-x}As$ is taken to be $1.425x-0.9x^2+1.1x^3$. Sixty percent of this is taken to be in the conduction band. The effective mass is related to the GaAs mass by $m^*(x)=0.0665 + (0.0835\Delta G/1.625)$.

Using the framework set up in the previous paragraph it is relatively easy to calculate the well width for which the n=2 state becomes unbound for a $GaAs/Al_xGa_{1-x}As$ quantum well system with any value of x. The results of such a calculation are shown in the upper half of figure 6. The maximum Al fraction considered corresponds approximately to that at which $Al_xGa_{1-x}As$ becomes indirect gap. In order to fabricate a quantum well infra red detector one has to grow a structure with a quantum well width less than the critical width for the particular aluminium content. The minimum energy required to "photoionize" the quantum well can be calulated by solving the Shrodinger equation and obtaining an equation for the bound states very similar to equation (5) but with non parabolic dispersions and energy dependent effective masses. The results of this equation are shown in the lower half of figure 6.

In practice if one wished to specify a structure to be grown as a quantum well detector one would be best advised to have a well width which was a few Angstroms narrower than the minimum value determine here in order to ensure that the n=2 state has become "well and truly" unbound. The results of a calculation of the threshold energies for various detector configurations with well widths less than the critical values of figure 6 are shown in figure 7.

Equations (10) and (11) provide a means of determining the in-plane masses of the two different subbands mentioned in section 2(iii). A more sophisticated calulation of the absorption lineshape would procede by using the nonparabolic dispersions of equations (10) and (11) in equations (1) to (9) to calculate the absorption lineshape starting from a fixed wavevector in the initial state and then convolving this with a suitable broadening function. (This is a Fermi function with its energy scale squashed by the factor $(1-m_1/m_2)$.)

This additional broadening of the line width results in a peak absorption coefficient which is a factor of three to four lower than that shown in figure 5., i.e. $\approx 10^6\ m^{-3}$.

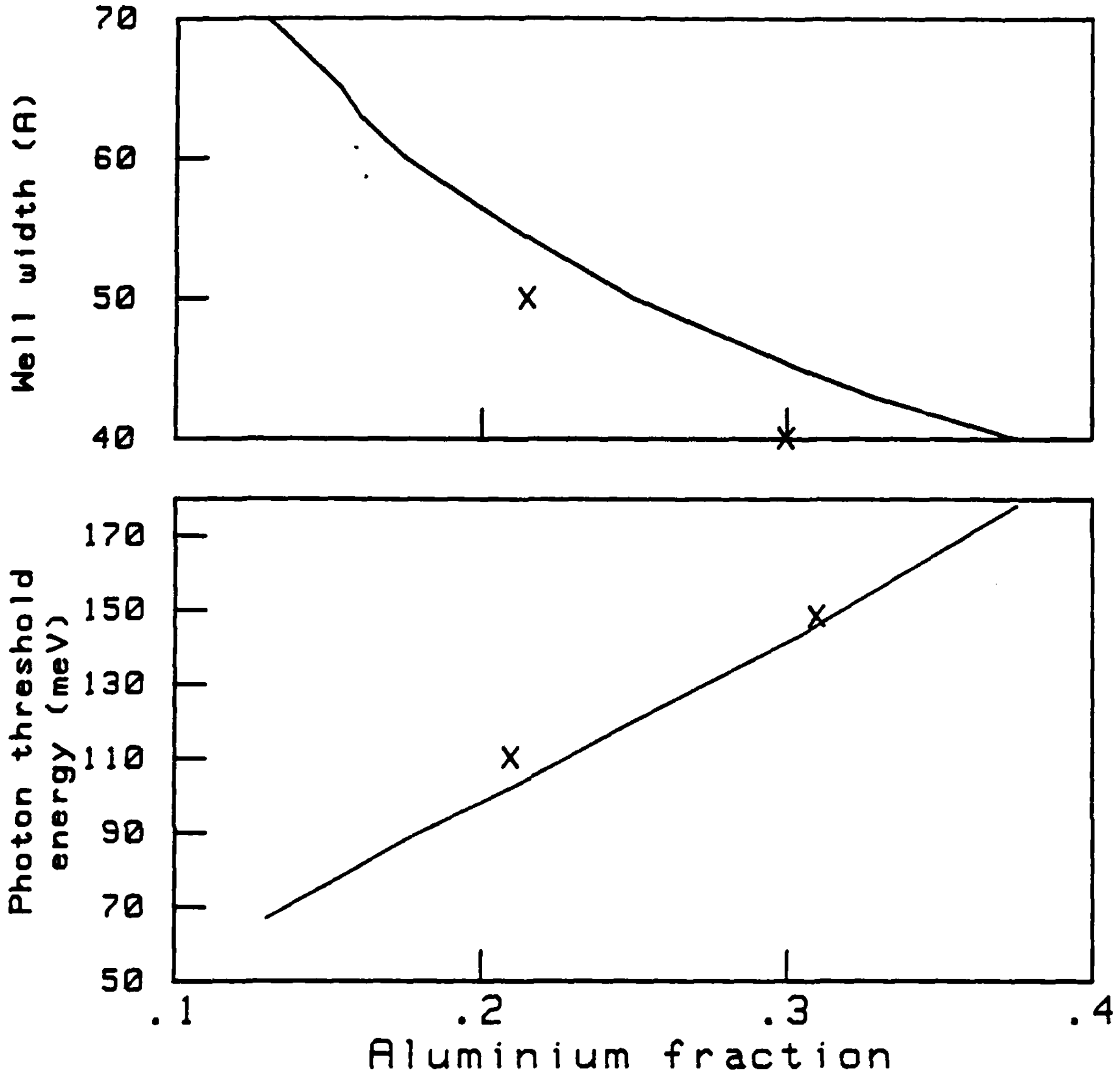

Figure 6 The "critical" thickness of quantum well for which the n=2 state just becomes unbound and the photoionization threshold energy at this critical thickness as a function of aluminium content. (Non parabolicity is taken into account.)

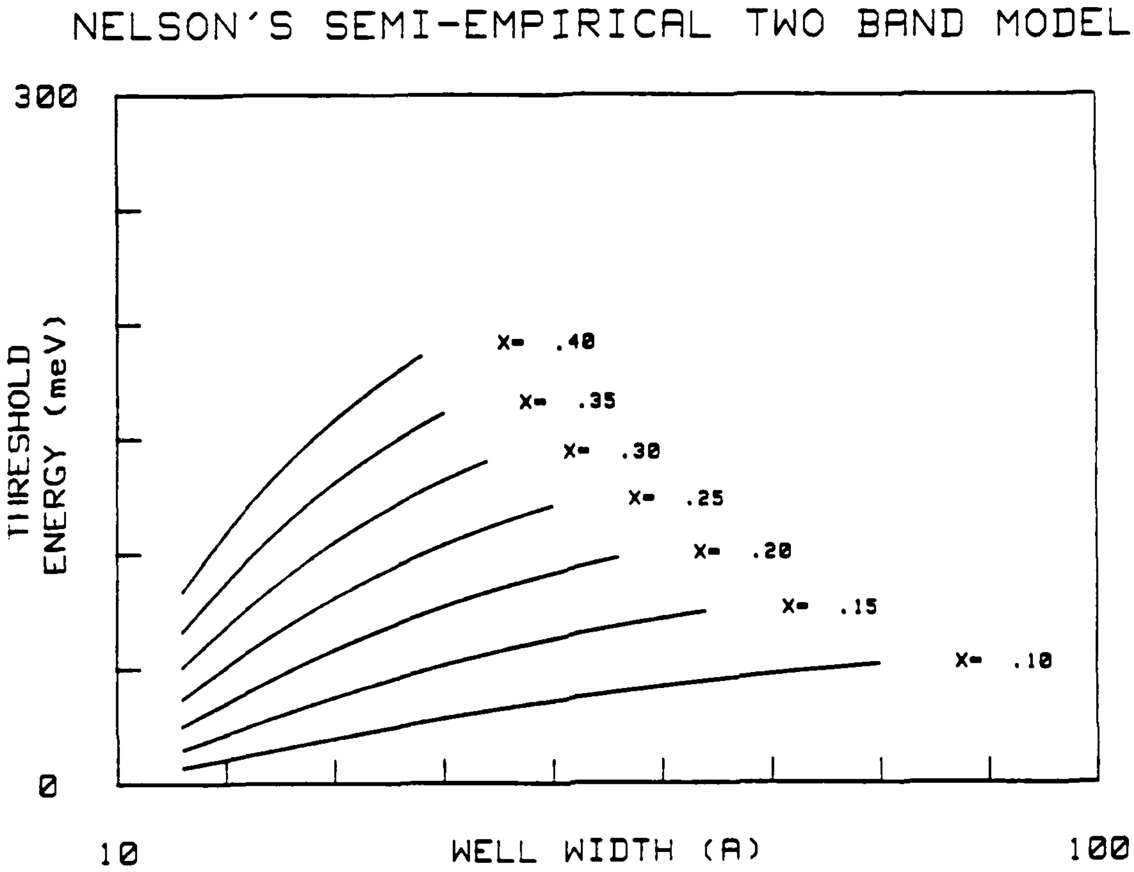

Figure 7 The photoionization threshold energy as a function of well width for various aluminium contents. The lines stop at the well width where the n=2 state becomes bound.

This means that a detector structure containing 50 A wide wells doped at a level of 10^{24} m^{-3} needs to contain 100 wells in order to be one absorption length thick. Alternatively only 50 wells are needed if the doping level is raised to $2x10^{24}$ m^{-3}.

We are now in a position to design a detector with a given threshold energy. We wil choose a threshold energy of 100 meV. A convenient, (but by no means unique, well width is 50 A. Reference to figure 7 shows that an aluminium fraction of 21.5% will give the required threshold energy.

(The non uniqueness of this combination of properties is illustrated by reference 2. Levine et al have designed a detector with a threshold energy of 100meV by using a well width of 38 A and $Al_xGa_{1-x}As$ with x=.25. This is still consistent with figure 7.)

The barrier thickness must be chosen to reduce tunnel currents to an acceptable level. Empirically 500 A appears to be an acceptable value when x=.215. A sufficient number of wells must be included in the structure to give good quantum efficiency. As indicated above 50 is a reasonable number if the doping level is 2 x 10^{24} m^{-3}. In order to contact the structure thick contact layers of heavily doped GaAs are used.

In summary, a possible detector structure designed to work with a 100 meV threshold energy would consist of: a semi-insulating GaAs substrate, 1 μm of heavily doped n-type gallium arsenide, 500 A of $Al_xGa_{1-x}As$ with x=.215, 50 repeats of the unit 50 A n-type GaAs and 500 A AlGaAs and a 1 μm thick capping layer of GaAs.

5 Conclusions

This note has shown how to design a quantum well infra red detector with controlled optical properties. The experimental verification of these rules will be the subject of a subsequent note as will be a discssion of the noise properties of these detectors.

References

1 B F Levine, C G Bethea, G Hasnain, J Walker and R J Malik, Appl. Phys. Lett. 53 296 1988.

2 B F Levine, G Hasnain, C G Bethea and N Chand, Appl. Phys. Lett. 54 2704 (1989).

3 C G Bethea, B F Levine, G Hasnain, J Walker and R J Malik, J. Appl. Phys. 66 963 (1989)

REPORT DOCUMENTATION PAGE

DRIC Reference Number (If known) ....

Overall security classification of sheet ....Unclassified...

(As far as possible this sheet should contain only unclassified information. If it is necessary to enter classified information, the field concerned must be marked to indicate the classification eg (R), (C) or (S).

Originators Reference/Report No.	Month	Year
MEMO 4363	FEBRUARY	1990

Originators Name and Location
RSRE, St Andrews Road
Malvern, Worcs WR14 3PS

Monitoring Agency Name and Location

Title
QUANTUM WELL INFRARED DETECTORS I:
SOME CALCULATIONS OF THEIR OPTICAL PROPERTIES

Report Security Classification	Title Classification (U, R, C or S)
UNCLASSIFIED	U

Foreign Language Title (in the case of translations)

Conference Details

Agency Reference	Contract Number and Period

Project Number	Other References

Authors	Pagination and Ref
KANE, M J	17

Abstract

The quantum well infra-red detector is a new kind of infra-red photon detector that can be made to work in the wavelength range 5 to 20 μm. This memorandum describes some theoretical calculations which illustrate the mode of operation of this detector. The initial part of the memo describes qualitatively the manner in which a quantum well system can be made into an infra-red photoconductor and illustrates the optical processes in such a device with some calculations of the properties of an idealised system. The second half of the memo concentrates on including some of the corrections necessary to give an accurate description of a real quantum well system and presents the design rules necessary to give a detector with a specified threshold photon energy.

Abstract Classification (U,R,C or S)
U

Descriptors

Distribution Statement (Enter any limitations on the distribution of the document)

UNLIMITED

580/48